

## Article

# A Systematic Heat Recovery Approach for Designing Integrated Heating, Cooling, and Ventilation Systems for Greenhouses

Mohsen Ghaderi, Christopher Reddick and Mikhail Sorin \*

Department of Mechanical Engineering, Université de Sherbrooke, 2500 Boul. de l' Université,  
Sherbrooke, QC J1K 2R1, Canada; gham2203@usherbrooke.ca (M.G.); j.christopher.reddick@usherbrooke.ca (C.R.)  
\* Correspondence: mikhail.v.sorin@usherbrooke.ca

**Abstract:** Ventilation heat loss is one of the most important factors contributing to energy performance of greenhouses. This paper suggests a systematic method based on dynamic pinch analysis (PA) to design an integrated heating, cooling, and ventilation system that uses ventilation waste heat in a cost-effective and energy efficient way. A heat recovery system including an air handling unit, borehole thermal storage, and a heat pump is proposed to investigate all heat integration scenarios for an entire year. In the first step, the heat integration scenarios are reduced to a few typical days using a clustering technique. Then, a generic methodology for designing a heat exchanger network (HEN) for a dynamic system, ensuring both direct and indirect heat recovery, is presented and a set of HENs are designed according to the conditions of typical days. Afterwards, the best HEN design is selected among all design alternatives using a techno-economic analysis. The whole procedure is applied to a commercial greenhouse and the best HEN configuration and required equipment sizes are calculated. It is shown that the best-performing design for the greenhouse under study produces primary energy savings of 57%, resulting in the shortest payback period of 9.5 years among all design alternatives.

**Keywords:** greenhouse; pinch analysis; heat exchanger network; clustering; techno-economic



**Citation:** Ghaderi, M.; Reddick, C.; Sorin, M. A Systematic Heat Recovery Approach for Designing Integrated Heating, Cooling, and Ventilation Systems for Greenhouses. *Energies* **2023**, *16*, 5493. <https://doi.org/10.3390/en16145493>

Academic Editors: Yuehong Su, Jae-Weon Jeong, Jingyu Cao, Devrim Aydin, Michele Bottarelli and Carlos Jimenez-Bescos

Received: 22 June 2023  
Revised: 12 July 2023  
Accepted: 18 July 2023  
Published: 20 July 2023



**Copyright:** © 2023 by the authors. Licensee MDPI, Basel, Switzerland. This article is an open access article distributed under the terms and conditions of the Creative Commons Attribution (CC BY) license (<https://creativecommons.org/licenses/by/4.0/>).

## 1. Introduction

As demand for greenhouse agriculture continues to grow, reducing the associated energy cost has become a major challenge. The greenhouse industry is an energy-intensive sector and the energy cost can be as high as 70–85% of the total operating cost in a typical greenhouse [1]. The primary reason for this is the significant climate control energy demand accounting for up to 90% of the total energy requirements [2]. The high energy consumption is mostly due to the energy losses associated with inefficient practices for maintaining greenhouse cultivation conditions. Currently, natural ventilation through opening the roof vents is common practice to control the humidity level inside greenhouses. However, this incurs significant heat loss from greenhouses during the heating season and is among the biggest challenges in greenhouse energy management, particularly in cold regions [3]. Excessive heat loss can be partially mitigated through forced/mechanical ventilation by removing undesired energy exchange due to the lack of control over the airflows in natural ventilation. However, mechanical ventilation introduces an extra energy cost due to the electricity consumption of fans, and as a result, a combination system of forced ventilation and natural ventilation would offer the most economically viable solution [4,5].

In addition, heat recovery systems, which can capture and reuse heat from ventilation air, can be an effective strategy in reducing energy consumption. Various technical options exist for recovering thermal energy from ventilation systems, which can be categorized into two main groups: passive and active recovery systems. Passive systems refer to different configurations of air-to-air heat exchangers (AHXs), enabling direct heat recovery without any need for an external device such as a heat pump. The utilization of AHXs

in greenhouse ventilation systems has proven to provide considerable energy efficiency benefits. Coomans et al. [6] compared a semi-closed greenhouse equipped with a recuperation stage with a naturally ventilated greenhouse. It was observed that employing a heat recovery device enhances the energy efficiency of the greenhouse by 28%. Maslak [7] studied the energy saving potential of a non-hygroscopic rotary air-to-air heat exchanger for a tomato greenhouse and a 17% energy efficiency improvement was achieved. Rousse et al. [3] investigated the performance of a low-cost air-to-air heat exchanger unit for a greenhouse located in Quebec. It was shown that the application of multi-pipe counterflow heat exchangers is favorable in small scale within the range of 0.5–1 ACH.

On the other hand, in an active recovery system, heat recovery is conducted through a thermal cycle created by a heat pump. The exhaust air heat pump (EAHP) is increasingly gaining popularity as an innovative technology in modern ventilation systems. In an EAHP, heat is recovered from the warm exhausted air by an evaporator and is delivered to a condenser to preheat the supply air during winter. Currently, EAHPs are being widely used in many energy efficient buildings and are used in almost all newly built family houses in Europe [8]. However, due to the limited capacity of EAHPs, auxiliary devices are often needed to maximize heat recovery potential [9]. Li et al. [10] evaluated the performance of an AHX coupled with an EAHP under different climatic conditions. It was concluded that the integration of an AHX always reduces the annual energy consumption of the heating, cooling, and air conditioning (HVAC) system. Perone et al. [11] introduced and optimized the heating performance of a prototype forced ventilation system using a combination AHX/heat pump for a greenhouse. The results showed superior performance of the system in terms of energy efficiency and temperature control in the greenhouse. Shuailing Liu et al. [12] proposed a more complex integrated system that incorporates both a pump-driven loop heat pipe and an EAHP to improve energy efficiency in cold regions. The temperature effectiveness of the integrated system was calculated to be 52.9% higher than that of the heat pump alone. A comprehensive literature review reveals that existing heat recovery technologies are primarily based on direct heat recovery, and indirect heat recovery through thermal energy storage is completely overlooked, which prevents the whole heat recovery potential from being fully realized. In addition, current studies on heat recovery predominantly concentrate on analyzing heat recovery devices and there is a lack of a comprehensive and systematic approach for sizing and designing the configuration of the heat recovery system, especially in more complex units.

The heat integration technique based on pinch analysis (PA) has been a well-established method in the process industry for many years for designing and optimizing heat recovery systems [13]. In general, a PA problem starts with an energy targeting phase to determine the maximum heat recovery possible and is followed by matching an optimal heat exchanger network (HEN) that connects heat sources and sinks in the most energy efficient way. In recent years, some attempts have been made to extend the applicability of the pinch-based design approach to HVAC systems. For example, in the study by Miseviciute et al. [14], PA was employed to analyze and redesign the HEN of a building's ventilation system. It was demonstrated that the building's energy demand could be reduced by approximately 26% through heat integration compared to the reference system without heat recovery. Reddick et al. [15] further developed this idea by using steady-state pinch analysis to integrate waste heat into a building's heating system. However, the impact of dynamic behavior of the waste heat source, and ever-changing temperature values, were not reflected in this study, which could raise serious questions about the relevance of the steady-state pinch method for such applications. Hosseinnia et al. [16] proposed a dynamic pinch strategy that uses instantaneous energy targeting to handle changes in the heat capacity of waste heat and other renewable sources. Dynamic PA also allows for integration scenarios using thermal energy storage by accounting for charging/discharging timing. This method was successfully applied to the integration of gray water waste heat, and sizing a hybrid solar-assisted heat pump with seasonal heat storage for a residential building [17].

Given the fact that any temperature change in heat sources and sinks (hot/cold streams) can alter the HEN structure, designing a HEN to completely meet dynamic energy targets is not a trivial task. Superstructure-based mathematical programming is a widely used approach for HEN design. However, the superstructure, which represents all potential matches between hot and cold streams, may introduce a huge number of variables for a dynamic system, making this method complex and impractical for dynamic heat integration. Therefore, a simple yet effective HEN design method is required to consider the variability in temperatures and heat capacities of the streams.

The present paper presents a heuristic method to design a cost-efficient HEN for a set of dynamic streams. This generic method is then applied to a case study greenhouse to design an integrated climate conditioning system enabling ventilation waste heat recovery. This study is a continuation of our previous work [18] in which heat integration was successfully accomplished by defining the greenhouse heating, cooling, and ventilation systems as a set of streams. A clustering technique, as the cornerstone of the method, was proposed to limit the problem size from a year to a few typical days. This paper addresses the HEN design problem for the obtained typical time periods and discusses the selection criteria of the best configuration of an integrated greenhouse climate conditioning system. Furthermore, the key techno-economic aspects and potential profitability of different heat integration schemes based on different typical seasonal weather conditions of a year are examined. To the best of our knowledge, this is the very first attempt to apply dynamic PA for the design of greenhouse climate conditioning systems. This innovative approach opens up new possibilities for designing greenhouses that effectively utilize and harness the extremely dynamic ventilation waste heat. Aside from novelty in application, this paper presents a generic heuristic method for identifying the most efficient and economical heat integration scenario, maximizing heat recovery and minimizing total cost for any dynamic energy system. Furthermore, the proposed method is more easily applicable and practical for determining equipment sizes and the HEN configuration than complex superstructure-based mathematical programming. This research lays the foundation for future advancements in greenhouse design and highlights the potential of dynamic PA as a valuable tool in finding sustainable and energy-efficient design alternatives.

## 2. Case Study Description

A 1125 m<sup>2</sup> four-span commercial greenhouse located in Saskatoon is selected as a case study [19]. In the original design, which is referred to as the reference case hereafter, the greenhouse heating is supplied by a natural gas (NG) boiler connected to a heating distribution circuit including a set of fan coil units (FCU loop). Furthermore, the cooling and dehumidification loads are met through air exchange by natural ventilation. In the present study, the feasibility of enhancing the reference climate control system's performance by integrating ventilation waste heat is examined. The basic idea is to integrate the natural ventilation system with a mechanical ventilation system equipped with a heat recovery heat pump and heat storage. So, the proposed system is composed of (1) an air handling unit (AHU) to accommodate an efficient heat exchanger network to collect the ventilation waste heat, (2) borehole thermal energy storage (BTES) that acts as seasonal energy storage, allowing the waste heat to be stored during the warmer months and then used during the colder months, and finally, (3) a heat pump. Figure 1 shows the streams representing the suggested system annotated from 1 to 10 and the potential heat integration schemes in greenhouse heating and cooling modes. A detailed description of the streams can be found in our previous work [18] and is not reiterated here. Table 1 briefly presents the specifications of all streams in the system, including the source and target temperatures, as well as the heat capacity ( $CP = \dot{m} \cdot c_p$ ) for each stream. Note that the streams associated with the water flow passing through the FCUs and the air passing over the coils (streams 9 and 10) are excluded from analysis since they are already matched via fan coil heat exchangers and cannot be integrated in any other way (see Figure 1). Similarly, the water/glycol mixture flow supplied to the boreholes (stream 8) is disregarded (this stream can only

exchange heat with the ground through borehole heat exchangers). The returning flow from boreholes are represented by two non-coexisting streams depending on whether the boreholes are charging (stream 5) or discharging (stream 6) since the working temperature of the BTES is different in heating and cooling modes (see Table 1). Furthermore, “hot and cold utilities” are supplied by a natural gas boiler and natural ventilation, respectively.

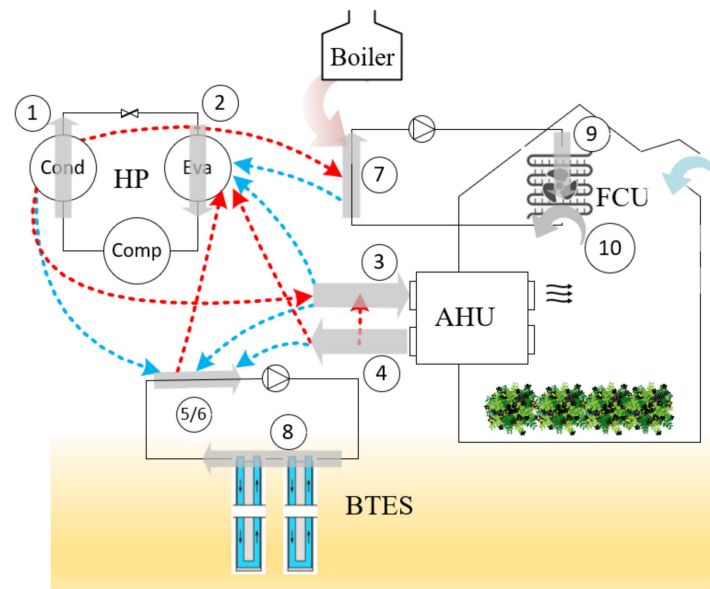


**Figure 1.** Schematic of heat integration schemes of the proposed climate conditioning systems for the greenhouse (red and blue colors are used for heating and cooling and gray arrows represent the streams).

**Table 1.** Stream properties.

No.	Stream Name	Description	Hot/Cold	Fluid	$T_s$ (°C)	$T_t$ (°C)	CP (kW/°C)
1	HP_Cond	refrigerant flow passing through the condenser of HP	H	R152a	78.7	45	constant
2	HP_Eva	refrigerant flow passing through the evaporator of HP	C	R152a	−10	−5	constant
3	Supply air	airflow delivered to the greenhouse using AHU	H/C	air	$T_{out}$	$T_{AHU}$	dynamic
4	Exhaust air	airflow rejected from the greenhouse using AHU	H	air	$T_{in}$	$T_{out}$	dynamic
5	BTES <sub>ch</sub>	BTES return flow during BTES charging (cooling mode)	C	water/glycol	10	15	dynamic
6	BTES <sub>d</sub>	BTES return flow during BTES discharging (heating mode)	H	water/glycol	0	−5	dynamic
7	Heating loop	FCU loop return flow	C	water	30	40	dynamic

### 3. Methodology

Figure 2 shows the overview of the design methodology, which is structured into four sequential steps, namely, data preparation, energy targeting, HEN design, and techno-economic analysis. This work is a sequel to our previous study [18] in which the former two steps were discussed in detail. In summary, to begin with, the required input data to fully define the streams listed in Table 1 (i.e., hourly thermal loads, ventilation rate, relative humidity, and temperature profiles) were generated using a greenhouse climate model. Then, dynamic PA was introduced by dividing the total time into smaller time intervals in which steady-state conditions could be achieved. So, the energy targeting was performed by constructing composite curves (CCs) based on the collected data on an hourly scale to provide sufficient temporal resolution to capture key characteristics in profiles of

temperatures and heat capacities. Furthermore, in order to reduce the data to a manageable size, the input data were clustered into a number of groups (i.e., 10 clusters plus two extreme heating/cooling days) containing similar days in terms of daily patterns of thermal loads. For each cluster, a “typical day” (TD), which is the most representative day of the cluster (i.e., centroid of the cluster), was selected and a weight was assigned denoting the number of days in the cluster. In fact, by using typical days, the heat integration problem has been successfully limited to only a few typical scenarios that are repeated during the year. It should be mentioned that the detailed description of the clustering process, including finding the optimum number of typical days, accuracy of clustering, and algorithm selection have already been discussed [18] and are not reiterated here. Furthermore, to facilitate interpretation of the results in this study, all chosen typical days are categorized into three main climatic conditions. TD1 to TD4 represent “very cold” days (no cooling) of the year, which are typical of winter days. TD5, 6, 8, and 9 are typical fall or spring days with cold nights and relatively warm days, which are labelled as “mild-cold” days. Finally, TD7, 10, 11, and 12 describe “warm” days of the year. Figure 3 shows the selected typical days and corresponding typical climates for the greenhouse under study.

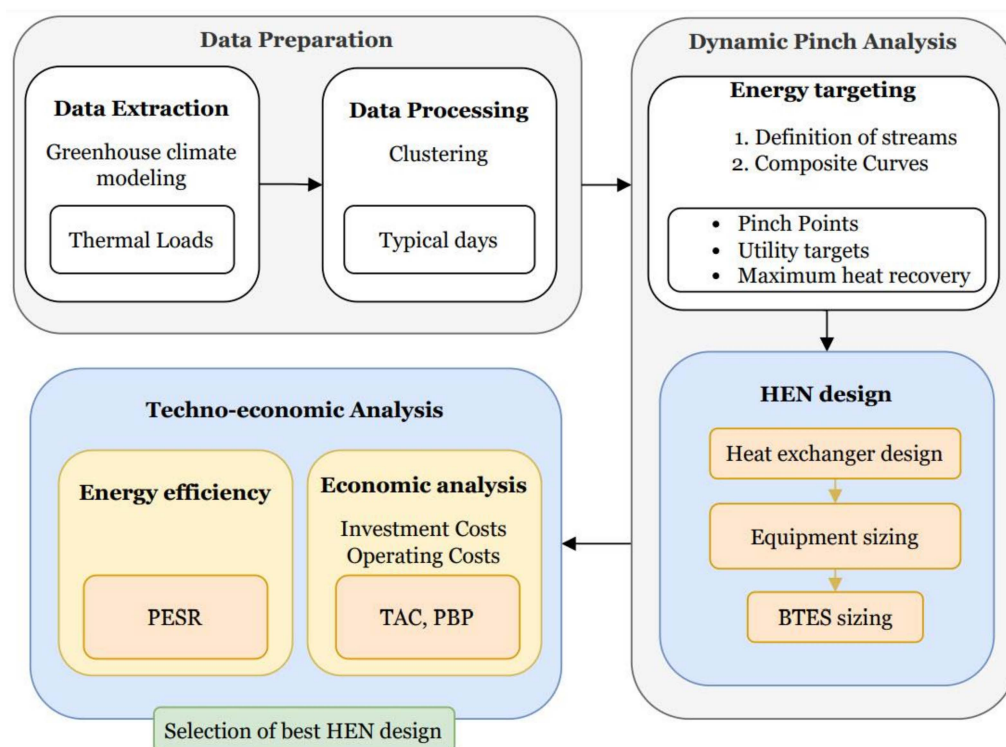


**Figure 2.** Design methodology structure (the non-colored sections were discussed in our previous paper [18]).

This work is built on the energy targeting results derived from the composite curves for the selected typical days. First, a step-by-step approach to design, combine, and merge all hourly-based HENs into a few HEN structures corresponding to the available typical days is described. Once the HEN structures are set for all TDs, the equipment sizing is carried out. Then, a holistic techno-economic analysis is performed to find the best design configuration for the greenhouse climate conditioning system. The present method not only provides a practical method to design a cost-effective HEN representing the best interconnection of system components, but also determines the equipment size and supports the decision-making process for the selection of climate control technologies for the greenhouse. In particular, the mechanical/natural ventilation ratio, electrification ratio of the reference system (i.e., HP/NG boiler capacity ratio), the structure of hybrid multi-source HP, and the required BTES size are the most important outcomes that can be directly

achieved from the proposed method without any need for complex and time-consuming superstructure-based mathematical programming. While the proposed methodology does not guarantee the global optimum for the HEN due to the heuristics involved, it could provide a promising solution by selecting one of the best local optimums among all those calculated for the most repetitive typical scenarios (i.e., TDs) in a year.

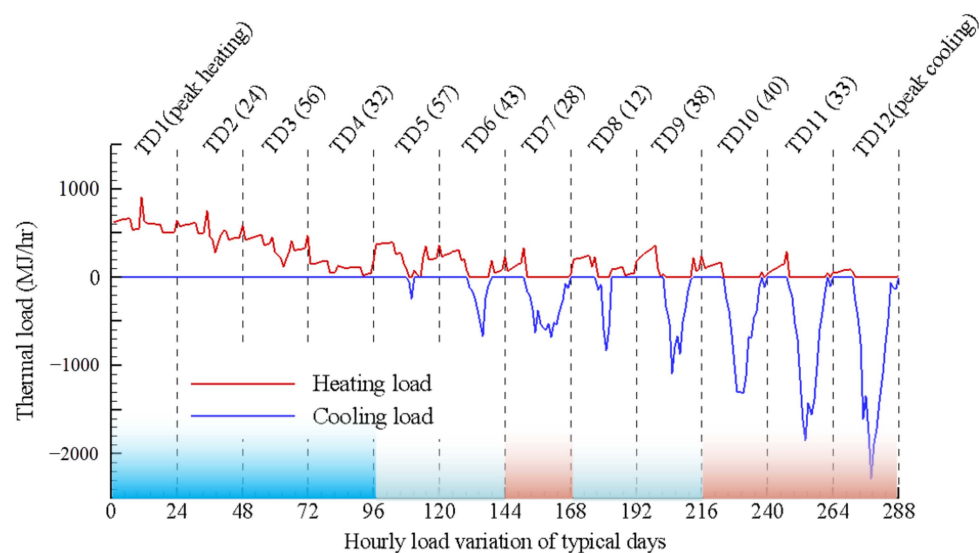


**Figure 3.** Selected typical days, their associated weights, and corresponding typical climates; blue color shows the typical winter days, light blue shows the typical mild-cold climate (transition days), and red color denotes the typical warm days [18].

### 3.1. HEN Design Strategy

The procedure of HEN design in this study is adapted from the general method used for batch process HEN synthesis [20]. In fact, each typical day is considered as a batch period with 24 equally sized time intervals. For each hour, a subnetwork, which is a heat exchanger network for that particular hour of the day, is designed based on the conventional grid diagram in which hot/cold stream matching is conducted using basic PA principles including CP inequality, stream splitting, and avoiding cross pinch heat transfer [21]. Once the hourly grid diagrams are built, the sizes of the various heat exchangers must be determined using the logarithmic mean temperature difference (LMTD) method. According to this method, the total heat transfer area for a given heat exchanger can be calculated as follows:

$$A = \frac{Q}{U\Delta T_{LMTD}} \left( \text{m}^2 \right) \quad (1)$$

where  $Q$  and  $\Delta T_{LMTD}$  represent the thermal duty and logarithmic mean temperature difference (LMTD) of the heat exchanger and can be extracted from grid diagrams.  $U$  is the overall heat transfer coefficient and is highly dependent on the type and geometric parameters of the heat exchanger. In the present study, three different heat exchanger types are involved: finned tube heat exchangers for air/water matches, corrugated plate heat exchangers for AHX, and plate heat exchangers for the evaporator and condenser of the HP. Accordingly, different thermal models have been developed to calculate the  $U$  value based on the heat exchanger type. The elaborate description of the mathematical modeling for the different types of heat exchangers under investigation is given in Appendix A. Finally, the overall heat exchanger network for each TD is made up by the combination of the corresponding subnetworks. It should be noticed that there might be some heat exchangers connecting the same stream pair in different subnetworks of a day. In this case, the largest area of all the shared heat exchangers in the subnetworks of the day is selected for the area size. As a result, there are 12 potential HEN designs corresponding to 12 typical days (including the hottest and coldest days of the year, i.e., TD1 and TD12)

maximizing heat recovery for their respective cluster. In the following section, the process of sizing the system components fulfilling the HEN requirements for each typical scenario will be described.

### 3.2. Equipment Sizing

For each TD, the HP is sized to supply the corresponding heating load entirely. As a result, no extra hot utility is required for all days of the cluster for which the HP is sized. So, the condenser capacity, evaporator capacity, and compressor nominal power consumption are calculated as follows:

$$\forall TD \quad \dot{Q}_{Cond}^{Design} = \frac{\sum_{h=1}^{24} \dot{Q}_h^{Load}}{HP \text{ working hours}} \quad (2)$$

$$\forall TD \quad \dot{W}_{comp}^{Design} = \dot{Q}_{Cond}^{Design} / COP \quad (3)$$

$$\forall TD \quad \dot{Q}_{Eva}^{Design} = \dot{Q}_{Cond}^{Design} - \dot{W}_{comp}^{Design} \quad (4)$$

The buffer tank is sized based on the worst-case scenario for the coldest day of the year (TD1). The details of HP cycle design and condenser-buffer tank matching were described in detail in the energy targeting phase in an earlier publication [18]. Knowing the heating capacity of the HP, the natural gas boiler capacity can be simply derived by subtracting the HP heating capacity from that of TD1 in which the HP is sized based on the coldest day of the year (i.e., HP-only scenario).

$$\forall TD \quad \dot{Q}_{Boiler}^{Design} = \dot{Q}_{Cond}^{Design,TD1} - \dot{Q}_{Cond}^{Design,TD} \quad (5)$$

### 3.3. BTES Sizing

The BTES sizing is based on the well-known ASHRAE/Kavanaugh model [22]. This model calculates the total borehole length using the following equation:

$$L = \frac{Q_a R_{ga} + Q_{eva} (R_b + PLF_m R_{gm} + F_{sc} R_{gst})}{T_g - \frac{T_{wi} + T_{wo}}{2} + T_p} \quad (6)$$

where  $R_b$ ,  $R_{ga}$ , and  $R_{gst}$  are the ground thermal resistances per unit length. PLF denotes the part-load factor during the heating month;  $T_g$  is the undisturbed ground temperature, which is 5 °C for the greenhouse location;  $Q_a$  and  $Q_{eva}$  represent the net annual average heat transfer to the ground and evaporator capacity, respectively.  $T_{wi}$ ,  $T_{wo}$  are the inlet and outlet borehole temperatures at design conditions. Finally,  $T_p$  represents the long-term ground temperature penalty caused by ground heat transfer imbalances. According to this equation, the heat imbalance during charging/discharging of the BTES can affect  $Q_a$  and  $T_p$ , which result in a larger BTES. Therefore, direct charging of the BTES through ventilation heat may improve the thermal balance and allow a smaller BTES to be selected. It also substantially reduces the electricity consumption required for active charging of the BTES using the HP.

The previous equation is used to determine the appropriate BTES size for all 12 proposed HEN configurations. To do so, the first step is to calculate the net annual average heat transfer to the ground,  $Q_a$ . Hence, given the HENs' layouts and the size of all heat exchangers, dynamic modeling of the HEN is performed for all scenarios using the Simulink platform. Yearly analysis of HEN yields the total heat recovered to charge the BTES, allowing for the calculation of  $Q_a$ . Then, the  $Q_{evap}$  and  $PLF_m$  are set based on the corresponding HP size and the BTES length is calculated. Note that  $Q_{evap}$  is the averaged heat extracted from the ground, which is calculated by deducting the contribution of the air evaporator from the nominal evaporator capacity.

### 3.4. Technoeconomic Analysis

#### 3.4.1. Economic Model

In order to compare the feasibility and profitability of the designed systems and facilitate the selection of the best scenario, an economic analysis is conducted. Capital and operating costs are two key factors that are considered in an economic assessment. Capital investment is mostly associated with the purchased equipment and can be estimated by summation of individual equipment costs. Table 2 summarizes the cost functions used to estimate initial expenses of the system under study.

**Table 2.** Capital cost correlations for system components.

Equipment	Component	Correlation	Ref
HP	PHX	$C_{PHX} = 805A^{0.74}$	[23]
	Compressor	$C_{Comp} = \frac{71.7\dot{m}}{0.92-\eta_{is}} PrLn(Pr)$	[24]
	Expansion valve	$C_{valve} = 114\dot{m}$	[24]
AHU	FTHX	$C_{FTHX} = 100A^{0.85}$	[25]
	Fan	$C_{Fan} = 1500\left(\frac{\dot{m}}{10}\right)^{0.36}$	[26]
	AHX	$C_{AHX} = 231A^{0.639}$	[23]
BTES	Borehole heat exchanger (drilling, installation, and pipe costs)	43 CAD/m	[27]
NG boiler	NG boiler	$C_{Boiler} = 205 Q_{Boiler}^{0.87}$	[28]

The operating cost is primarily composed of natural gas and electricity consumption expenses. The required hot utility provided by the NG boiler is obtained by applying a daily thermal balance to the buffer tank. So, the total yearly hot utility for each TD is calculated as:

$$Q_{Utility}^H = \sum_{d=1}^{365} \max\left(\sum_{h=1}^{24} \dot{Q}_h^{Load} - 24\dot{Q}_{Cond,TD}^{Design}, 0\right) \quad (7)$$

Furthermore, the electric utility is related to the electricity consumption of the HP, AHU fans, and circulation pumps that are expressed by the following equations:

$$E_{Utility}^{HP} = \left\{ \sum_{d=1}^{365} \left( \sum_{h=1}^{24} \dot{Q}_h^{Load} \right) - Q_{Utility}^H \right\} \frac{1}{COP} \quad (8)$$

$$E_{Utility}^{Fan} = \dot{V}_{air} \cdot \Delta P_{AHU} \quad (9)$$

$$E_{Utility}^{Pump} = \Delta P_{ref} \cdot L_{BTES} \cdot \dot{V}_{BTES} \quad (10)$$

In the above equations,  $\Delta P_{AHU}$  denotes the total pressure drop across the AHU,  $\dot{V}_{air}$  is the volumetric flow rate of the air,  $\dot{V}_{BTES}$  is the water/glycol flow rate circulated in the BTES, and  $\Delta P_{ref}$  is the head loss per meter of the borehole heat exchangers that is assumed to be 0.4 kPa/m based on the typical values often used in BTES design methodologies [27]. Note that the cost associated with the FCU recirculation pump is excluded from the analysis since it is common to all scenarios. The total operating cost is calculated as follows:

$$C^{OP} = Q_{Utility}^H \cdot C^{NG} + \left( E_{Utility}^{HP} + E_{Utility}^{Fan} + E_{Utility}^{Pump} \right) \cdot C^{elec} \quad (11)$$

where  $C^{NG}$  and  $C^{elec}$  are the electricity and natural gas prices and are set to 0.079 ¢/kWh and 0.028 ¢/kWh, respectively, based on averaged Canadian tariffs for businesses. In addition, annual maintenance costs are assumed to be 2% of the total capital cost [29].

### 3.4.2. Economic Performance Criteria

In order to determine the best trade-off between capital and operating costs, two different economic criteria are evaluated, namely, total annualized cost (TAC) and payback period (PBP). The TAC is obtained by summation of the operating costs and the annualized capital costs. The annualized capital cost is expressed as:

$$C_{anul}^{inv} = CRF \cdot C^{inv} \quad (12)$$

$$TAC = C_{anul}^{inv} + C^{op} \quad (13)$$

where, CRF is the capital recovery factor, which is a function of the interest rate and project lifetime. In this study, the interest rate and project lifetime are assumed to be 5% and 20 years, respectively.

$$CRF = \frac{i(i+1)^n}{(i+1)^n - 1} \quad (14)$$

The payback period (PBP) is defined as the required time to recover the initial investment. This index shows the ability of the system to refund the additional initial capital investment by a reduction in operating costs. In the present study, the NG boiler-only scenario is used as the reference heating system to calculate the PBP. So, the PBP for each HEN is given by:

$$PBP = \frac{C^{inv} - C_{ref}^{inv}}{C^{op} - C_{ref}^{op}} \quad (15)$$

### 3.4.3. Energy Saving Potential

To determine the energy efficiency of the suggested HEN designs, the energy savings achieved for each system with respect to the reference case are calculated. In that regard, the PESR (primary energy saving ratio) is used as the evaluation criterion to assess the energy savings potential. The PESR is defined as the ratio of the energy saved by introducing the HEN to the energy consumption of the reference system and is written as:

$$PESR^{HEN} = \frac{PE^{Ref} - PE^{HEN}}{PE^{Ref}} \quad (16)$$

where PE is the primary energy consumption (non-renewable sources) and is calculated by the summation of electricity and natural gas consumption for all components of the system.

## 4. Results

### 4.1. Configuration of HEN Design Alternatives

In this section, in order to better understand the problem of HEN design, the HEN layouts designed based on different TDs are investigated. Figure 4 compares CCs and grid diagrams for three different subnetworks corresponding to different times of TD5. As shown in this figure, the grid diagram configuration changes substantially depending on the availability of streams, instantaneous CP values, and temperature ranges. The selected times exhibit all possible HEN topologies that can occur during TD5. For the remaining hours of the day, the HEN topology is quite similar to any of these three subnetworks although heat exchanger duties differ.

As mentioned earlier, TD5 is a “mild-cold” typical day with a relatively moderate ventilation rate. Figure 5 illustrates the variations of weather parameters and their impact on the required heating and ventilation rate during TD5. At  $t = 0$  h, the greenhouse requires heating while the ventilation system is off. At this time the system acts exactly like a regular geothermal HP, meaning that the BTES is the only heat source available to the HP. However, around noon, at  $t = 13$  h, when radiation is maximum, the accumulation of solar energy inside the greenhouse causes a transition from heating to cooling mode and

the HP is switched off. In addition, the excessive moisture removal requirement arising from biological activity of the plants, intensified by high levels of radiation, forces the ventilation system to operate at its maximum capacity during this specific period. In this case, according to the grid diagram, two exchangers are required by which the exhaust air heat is first utilized to recharge the BTES (HX3) and then used to preheat outdoor frigid air (HX4) to a level meeting the cooling load. However, since the HP is off, part of the exhaust air energy that could have been reused by the HP is rejected to the environment and this is shown by an imaginary cold utility applied to the exhaust air stream in the grid diagram.

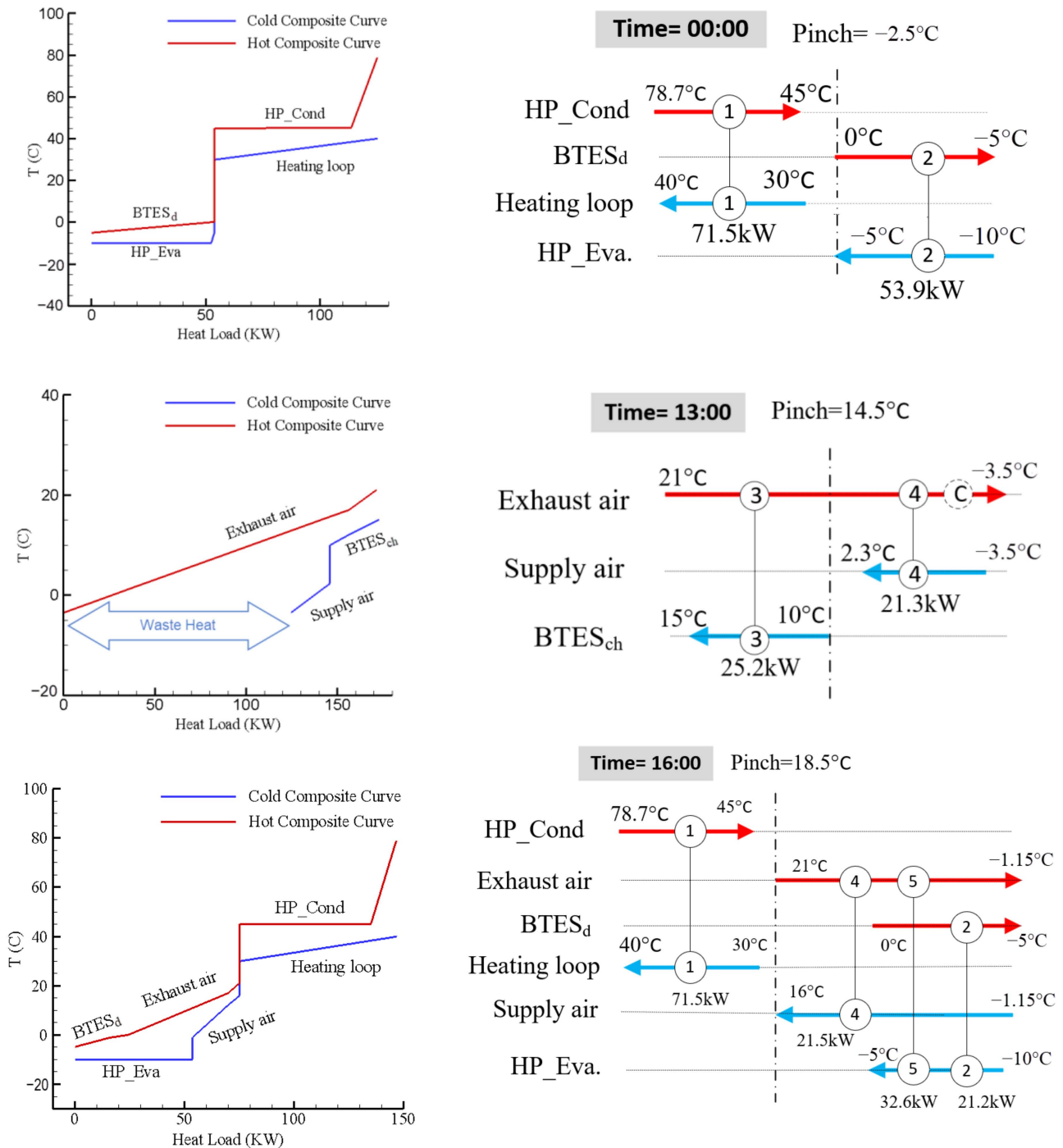


**Figure 4.** Composite curves and corresponding grid diagrams for different subnetworks during different times of the day (TD5); from top to bottom: t = 0 h, t = 13 h, and t = 16 h.

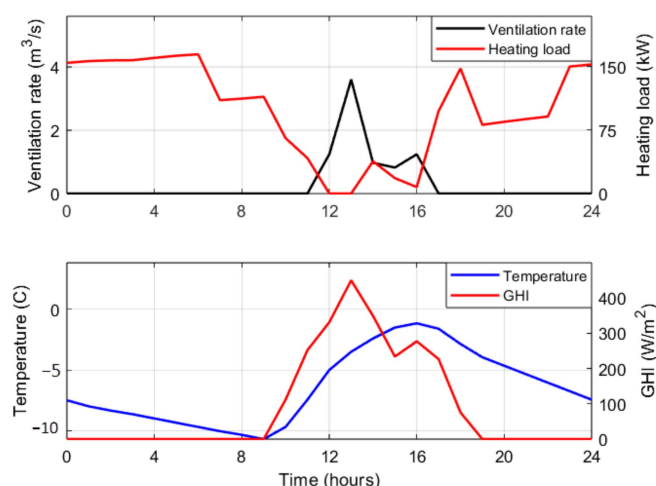


**Figure 5.** Variations of weather parameters and the required heating and ventilation rate during TD5.

As the radiation intensity gradually decreases, the greenhouse climate control system shifts back to heating mode and the HP switches on again ( $t = 14\text{--}17$  h). The designed HEN structures under this condition allow the HP to work in a hybrid mode, which means an auxiliary evaporator (HX5) must be placed downstream of the AHX (HX4) to capture the remaining heat from the exhaust air (see Figure 4,  $t = 16$  h). Since the AHX heat duty is relatively high to recover as much heat as possible from the exhaust air in heating mode, the remaining exhaust airflow heat content is not sufficient to fully supply the evaporation heat and a BTES evaporator is still required.

In order to better understand the stream interconnections in the network, the schematic configuration of the overall HEN for TD5 is shown in Figure 6. Given the fact that the sizing process was based on TD5 conditions, the composite curves show that there is no need for any hot utility during TD5. However, it is obvious that the HEN5 designed for a mild-cold day (i.e., TD5) requires additional hot utility when used for cold days (for example TD1). As a result, a backup NG boiler is used to provide the required “hot utility” to meet the heating demand for off-design operation of the system. In addition, since TD5 represents a winter day with a relatively low outdoor temperature, there is not a significant potential for supply airflow heat recovery and only one exchanger, HX4, is assigned to the supply side. In other words, AHX (HX4) is the only mechanism for generating cooling, resulting in an undersized system for the summer in terms of cooling capability. Thus, in order to meet the cooling loads in summer, the supplementary “cold utility” is provided by natural ventilation. It is worth mentioning that the flow capacity of the AHU, which is an important factor influencing the size of the AHU and its fans, is equal to the maximum required ventilation rate of the corresponding TD. This allows the AHU size to flexibly change during the design phase according to the TD conditions, which provides valuable design insights to determine the best balance between forced and natural ventilation.

To better analyze the structural changes of HEN architecture for different TDs, the HEN schematics for TD6 and TD7 are demonstrated in Figures 7 and 8. Since TD5 and TD6 are both typical mild-cold days, the overall arrangement of the system is relatively similar to that of TD5. The only change is a bypass channel with an extra heat exchanger at the exhaust side of the AHU. In fact, the network has been adjusted to handle a larger air flow rate with more heating capacity (i.e., CP). In this design, by changing the bypass ratio using shutters, the heat recovery priority may be shifted from direct heat recovery (HX4) to indirect heat recovery (HX6).

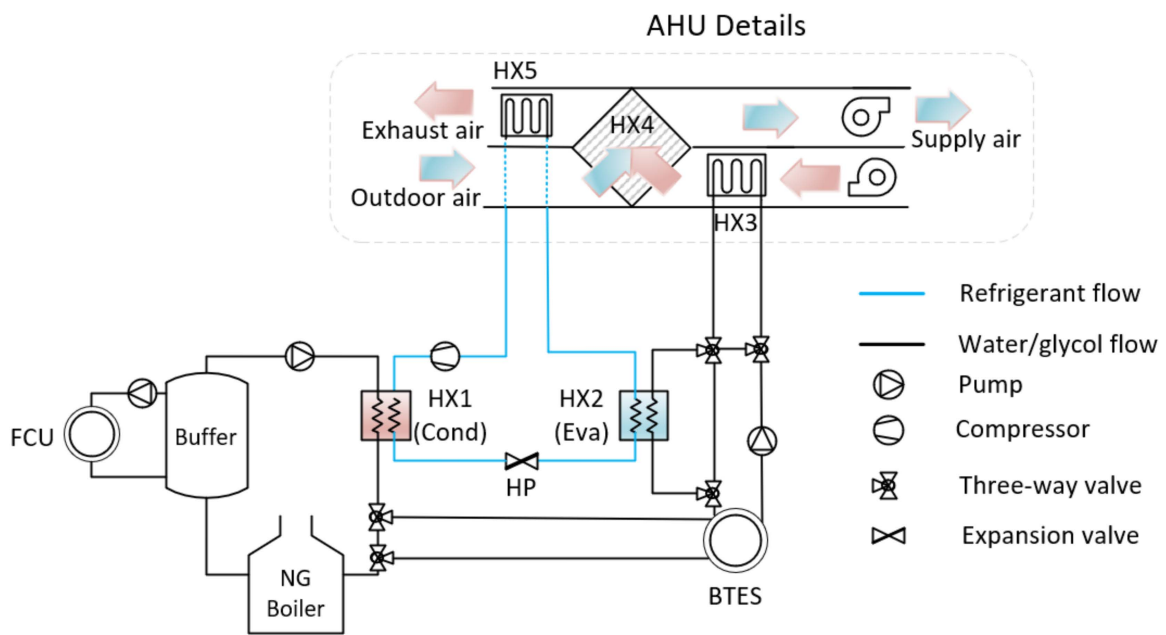


Figure 6. Schematic of the HEN design based on heat integration for TD5 (HEN5).

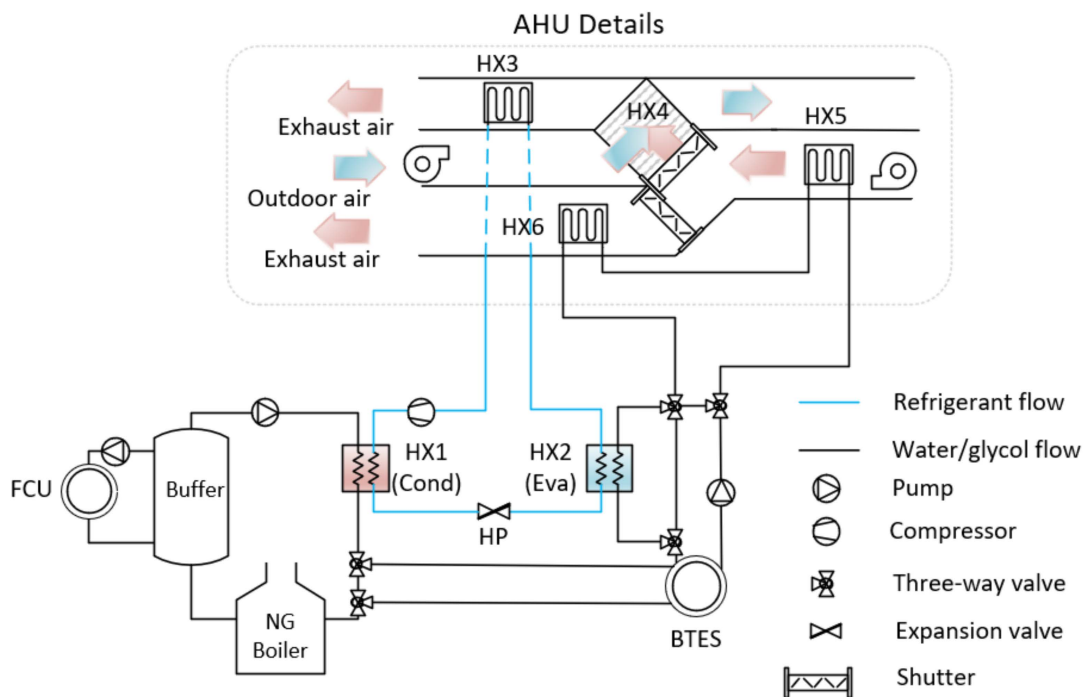


Figure 7. Schematic of the HEN design based on heat integration for TD6 (HEN6).

The AHU structure for typical summer days is quite different in some respects from those of winter days. As shown in Figure 8, for TD7, an additional heat exchanger (HX6) is positioned before the AHX to capture the incoming air excess heat and store it in the BTES. This can effectively improve the system capability in terms of cooling performance. Furthermore, adding a bypass on the supply side allows better control over the HX4 heat duty to achieve the desired outlet temperature for the air handling unit (AHU). Note that for the rest of the HENs represented by the typical “mild-cold” and “warm” days (i.e., TD8 to TD12) the HEN topology is similar to either TD6 or TD7, while they differ in terms of the size of both the heat exchangers and the equipment.

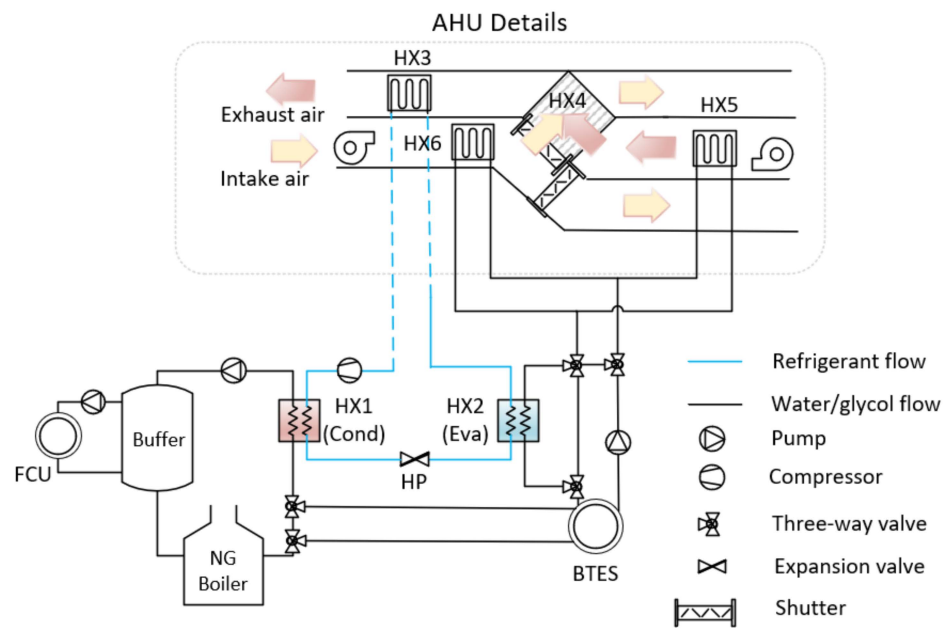


Figure 8. Schematic of the HEN design based on heat integration for TD7 (HEN7).

For typical “cold” days, TD1 to TD4, since the HEN structure is configured to accommodate a ventilation rate of zero, the AHU is excluded from the design, leading to comparatively simpler configurations. Figure 9 compares HENs 1 to 4 structures against the reference design. In the case of HEN1, the boiler is not required since the HP is sized based on the coldest day of the year. However, HENs 1 to 3 offer three design alternatives for combinations of a GSHP and a boiler based on the three most frequently occurring weather patterns of winter. It is important to note that all structures initially designed based on winter days without an AHU operate with a conventional natural ventilation system during summer. In the following section, the sizing results of the designed HENs will be discussed.

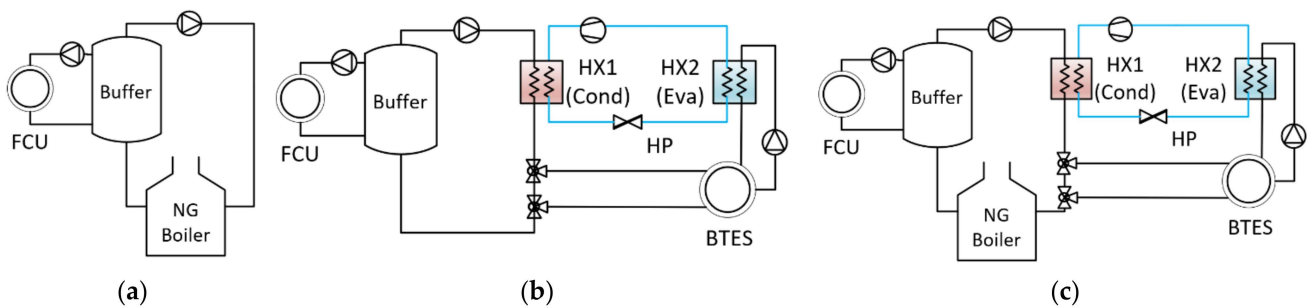


Figure 9. Comparison of (a) reference design with (b) HEN1 and (c) HEN2,3,4.

#### 4.2. Specifications of the Designed HENs

A detailed description of all 12 designed HENs is presented in Table 3. As discussed earlier, out of all design alternatives, four different scenarios (HEN1 to HEN4) are the hybridization of an NG boiler with a geothermal heat pump for a naturally-ventilated greenhouse. Without an air handling unit, PHXs in the HP cycle are the only heat exchangers of these HENs.

On the other hand, there are eight different HENs (HEN5 to HEN12) in which the ventilation waste heat is effectively integrated into the system using an AHU. In these cases, the HP features an additional air-source evaporator resulting in a considerably smaller BTES length than scenarios with regular GSHP (HEN1 to HEN4). Furthermore, for the typical days representing “warm” days of the year (TD7, 10, 11, and 12), since the HEN is configured to provide sufficient cooling capacity, there needs to be a large FTHX to collect a

significant amount of heat from the air delivered to the greenhouse. This is the main reason why the total FTHX heat transfer area is a large number for networks designed based on warm typical days.

**Table 3.** Specifications of the HENs designed for different typical days (Ref denotes the reference greenhouse).

No. of HEN	Ref	1	2	3	4	5	6	7	8	9	10	11	12
HP heating capacity (kW)	-	167.5	141.7	99.2	30.8	71.5	54	35.6	52.1	62.5	38.5	34	33.1
Boiler capacity (kW)	167.5	-	25.8	68.3	136.7	96	113.5	131.9	115.4	105	129	133.5	134.4
BTES total length (m)	-	4092	3671	2879	895	806	611	309	499	634	345	283	275
PHX (m <sup>2</sup> )	-	13.9	12.7	10.5	5.6	8.7	7.5	6	7.4	8.2	6.2	5.8	5.7
AHX (m <sup>2</sup> )	-	-	-	-	-	37	354	247	384	264	239	153	165
FTHX (m <sup>2</sup> )	-	-	-	-	-	54	110	274	107	132	410	569	588
Fans capacity (m <sup>3</sup> /s)	-	-	-	-	-	3	11.4	19.6	16	12.6	42.6	43	50

#### 4.3. Yearly Performance Analysis of the Designed HENs

Table 4 compares the performance of the design candidates calculated by dynamic simulation of each scenario over the course of an entire year. As can be seen, integration of ventilation airflows substantially decreases the ventilation losses and the HENs with higher forced/natural ventilation ratios have lower ventilation losses. The maximum reduction of 5% in the total heating demand can be achieved by a nearly fully-integrated ventilation system (HEN12). In addition, the results highlight that even for the smallest AHU designed for HEN5, almost 17% ventilation can be achieved through forced ventilation. The reason for this is that the daily ventilation peaks occur for only a few hours per day, and the typical ventilation rate is relatively low during the day. On the contrary, the largest AHU corresponds to HEN12 in which almost all ventilation peaks are covered by a forced ventilation system. Furthermore, the HP heating ratio values, defined as the thermal contribution of the HP to the overall heating, are reported in this table. As expected, the share of thermal energy provided by the HP is higher for the colder typical weather conditions in comparison to the others. Particularly, HEN5 has the highest HP contribution among all designs with an integrated ventilation system (i.e., TD5 to TD12).

**Table 4.** Yearly performance of the greenhouse (Ref denotes the reference greenhouse).

No. of HEN	Ref	1	2	3	4	5	6	7	8	9	10	11	12
Total heating (MWh)	481.4	481.4	481.4	481.4	481.4	475.9	469.6	472.4	468.6	469.1	460.8	457.7	457.6
Ventilation loss (kwh)	37,834	37,834	37,834	37,834	37,834	32,298	25,988	28,814	25,009	25,538	17,231	14,121	14,000
Forced/natural ventilation ratio	0	0	0	0	0	0.17	0.53	0.72	0.65	0.57	0.92	0.92	0.95
HP heating ratio	0	1	0.99	0.94	0.5	0.82	0.72	0.57	0.71	0.78	0.56	0.54	0.54

#### 4.4. Economic Analysis

In this section, the economic analysis results are presented to examine the practicality of all designed HENs. Figure 10 shows the investment cost breakdown of the proposed HENs. As can be seen, the BTES size is the most important factor contributing to the total investment cost, particularly for designs without an AHU (HEN1 to HEN4). The system has the maximum investment cost for the standalone GSHP sized according the coldest day of the year (HEN1). In this case, the initial capital investment is about seven times more than the reference case scenario. For all GSHP + boiler scenarios, namely, HENs 2, 3, and 4, the contribution of BTES to the total capital cost becomes relatively smaller as a larger boiler is integrated. However, a larger boiler may incur more operating cost and reduce the energy savings potential of the system. As shown in Figure 11, the total operating cost for HEN4 with a 137 kW boiler is about 17% more than that of the HEN1 with no boiler.

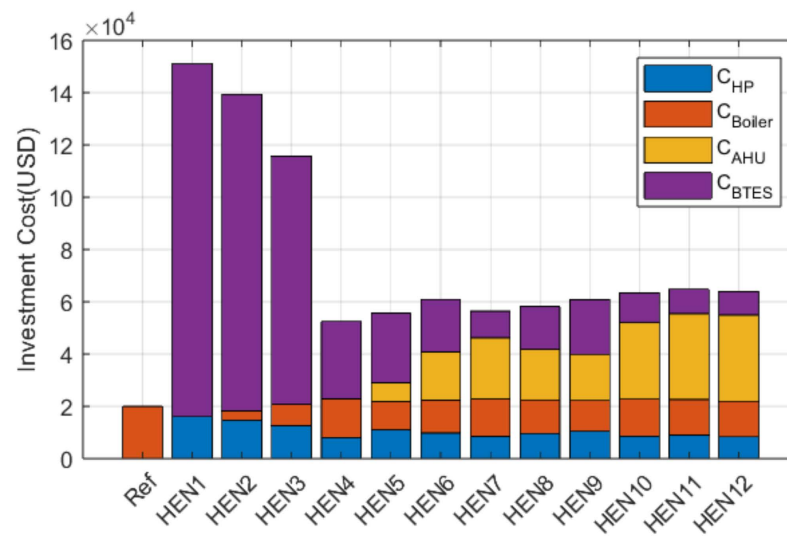


Figure 10. Breakdown of capital investment costs for the designed HENs.

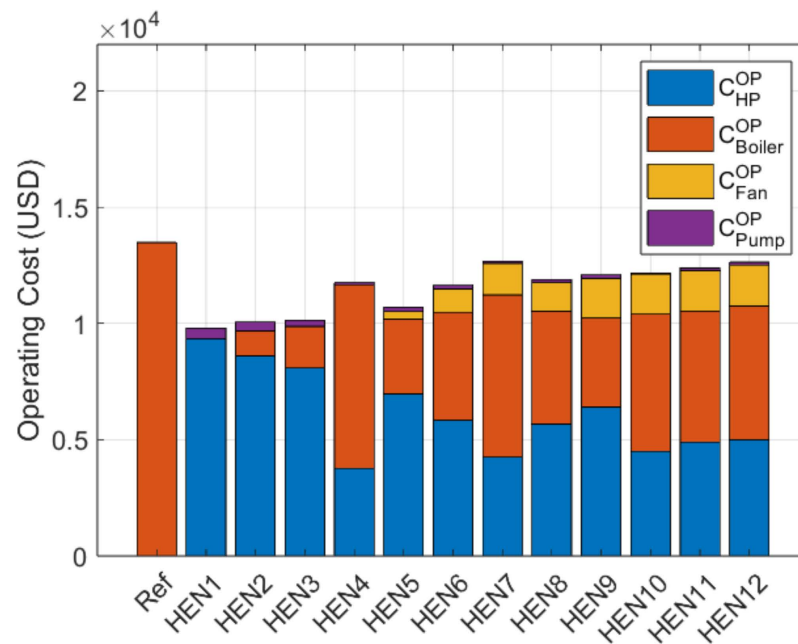
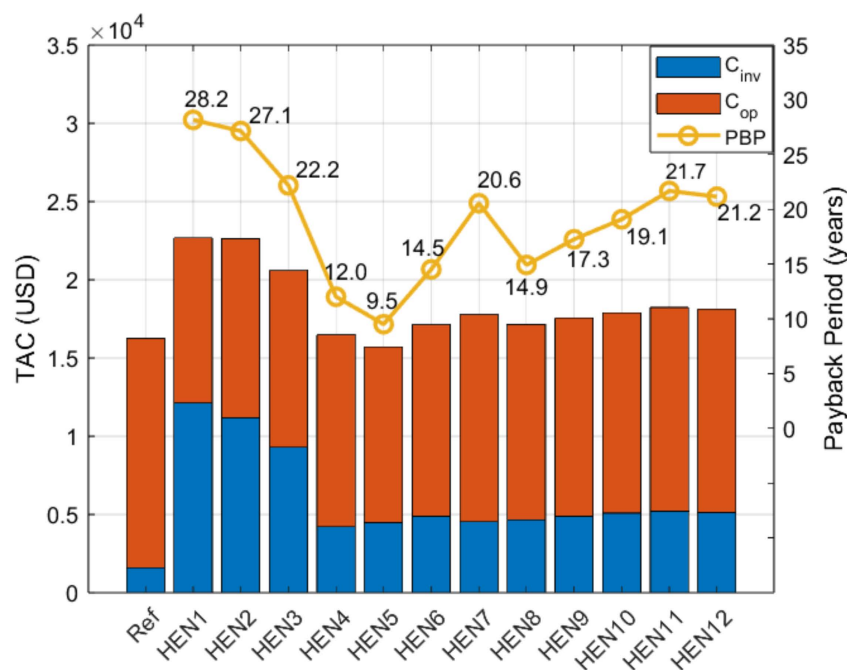


Figure 11. Breakdown of operating costs for the designed HENs.

On the other hand, for all designed HENs having an AHU (HEN5 to HEN12), the AHU unit cost accounts for a large proportion of the total investment cost. For HENs designed based on the warmer typical days of the year (HEN10, 11, and 12), the HP, BTES, and boiler are comparatively smaller, and the AHU investment cost contribution can be as much as 52% of the total investment cost. Note that a larger AHU requires larger fans resulting in increased operating costs. However, the contribution of fan energy cost ranges from only 3% to 13% of the total operating cost and the utility costs are still dominated by the energy consumption of the HP and boiler. Additionally, the operating cost related to the circulation pumps varies based on the BTES size and causes a slight increase in the total energy cost of the system.

The comparison of TAC and PBP values for different HENs is demonstrated in Figure 12. The HENs with a payback period beyond the project's lifetime (20 years) are deemed infeasible and therefore discarded.



**Figure 12.** TAC values and corresponding PBPs for the designed HENs.

The results clearly show that the conventional boiler-assisted GSHP designs (HEN1, 2, and 3) have long PBPs and are not economically competitive unless a relatively small HP is integrated (HEN4). This can be attributed to the significantly high initial costs due to the larger BTES. On the other hand, taking advantage of ventilation waste heat, HEN5–12 have relatively lower TAC values. Nevertheless, for HEN7, 11, and 12, each with a relatively large AHU, the AHU's capital cost and fan energy consumption offset the cost benefit from energy savings, resulting in infeasible PBPs. HEN5 has the lowest TAC of 15,720 USD/y, which is quite comparable to that of the reference case. In this case, effective integration of ventilation air reduces the operating cost by a large margin and can make HEN5 a cost-competitive design with a PBP of 9.5 years. In general, increasing the contribution of forced ventilation adversely affects the cost-effectiveness of the HEN.

#### 4.5. Selection of Optimal HEN Design

Table 5 presents the PESR values for all economically feasible HEN designs. According to this table, HEN5 is the best performing structure in terms of energy efficiency, which reduces the primary energy consumption by 57.3%. Having high energy efficiency with a short PBP of 9.5 years and almost the same TAC value as the reference design, HEN5 is selected as the best integrated network among all designed HENs.

**Table 5.** PESR values for different HENs.

No. of HEN	4	5	6	8	9	10
$PESR^{HEN}$	0.326	0.573	0.48	0.466	0.509	0.41

## 5. Conclusions

This paper investigated the possibility of ventilation waste heat recovery in greenhouses in the context of heat integration. A systematic methodology based on dynamic PA was developed to design an HEN with respect to economic and energy savings criteria. The proposed methodology was demonstrated based on a greenhouse climate conditioning system including a boiler, a heat pump, an air handling unit, and borehole heat storage. A number of typical days were identified through a clustering approach to reduce the integration scenarios to a manageable size, and as a result, 12 HENs were designed and

optimal equipment sizing and heat exchanger placement were determined. Finally, the best design was selected using a techno-economic analysis.

Thermal efficiency and economic performance of all design alternatives were examined using different criteria, including TAC, PBP, and PESR. The best performing design was found to be HEN5 with a TAC of 15,720 USD/y and a PBP of 9.5. The optimal system also demonstrated a significant energy saving potential of 57% with respect to the reference design.

In addition, it was shown that the BTES size is the most important factor contributing to the total system investment cost. The integration of ventilation air as a supplementary heat source for the HP decreases the required BTES size and thereby significantly reduces the investment cost. Although the reference design (NG boiler and natural ventilation) still has a lower initial cost by a large margin, the integrated systems showed superior performance over the reference design in terms of operating cost with the given energy tariffs. However, the operating cost benefit of a larger AHU unit, particularly for those scenarios associated with HENs designed for typical summer days (HEN7, 10, 11, 12), was diminished by the elevated fan energy consumption. In the case of the best design (HEN5), the integrated forced-ventilation contribution was found to be only 17% of the total ventilation requirement. So, it can be concluded that smaller AHUs are favored in terms of TAC. HEN5 also has the highest thermal contribution of the HP to the total heating requirements, being 82%.

Overall, there is a huge potential for heat recovery from ventilation air flows in greenhouses. Integration of ventilation waste heat into the greenhouse HVAC system not only allows for smaller BTES but also significantly improves greenhouse energy efficiency. Furthermore, dynamic PA has been proven to be a promising approach to addressing a highly dynamic heat integration problem. However, one important limitation of this method is that it does not provide a guarantee for achieving the optimal year-round design, as it primarily deals with local optima derived from the most frequently occurring scenarios throughout the year. Consequently, there is a need for further research to explore approaches that can address this limitation and enable the identification of global optimum solutions. One promising solution for future investigation is the integration of superstructure-based mathematical heat exchange network (HEN) design with clustering techniques. This integration could offer a more comprehensive analysis by considering a wider range of scenarios and their associated solutions, leading to a better understanding of the optimal design configurations for greenhouse climate-conditioning systems.

**Author Contributions:** M.G.: Conceptualization, methodology, investigation, validation, software, visualization, writing—original draft, writing—review and editing; C.R.: conceptualization, review and editing; M.S.: supervision, resources, methodology, funding acquisition, writing—review and editing. All authors have read and agreed to the published version of the manuscript.

**Funding:** The authors acknowledge the financial support of the Natural Sciences and Engineering Research Council of Canada for this project (RGPIN-2019-05826).

**Data Availability Statement:** Not applicable.

**Conflicts of Interest:** The authors declare no conflict of interest.

## Nomenclature

### Abbreviations

AHU	air handling unit
AHX	air-to-air heat exchanger
BTES	borehole thermal energy storage
CAD	Canadian dollar
CCs	composite curves
COP	coefficient of performance of heat pump
EAHP	exhaust air heat pump

FCU	fan coil unit
FTHX	finned tube heat exchanger
GHI	global horizontal irradiance ( $W/m^2$ )
GSHP	ground source heat pump
HEN	heat exchanger network
HP	heat pump
HX	heat exchanger
HVAC	heating, cooling, and air conditioning
NG	natural gas
PA	pinch analysis
PBP	payback period
PESR	primary energy saving ratio
PHX	plate heat exchanger
TAC	total annualized cost
TD	typical day
Subscripts	
air	airflow passing through AHU
annul	annualized
ce	cold stream outlet
ci	cold stream inlet
cond	condenser of heat pump
comp	compressor of heat pump
eva	evaporator of heat pump
g	gas/or ground
he	hot stream outlet
hi	hot stream inlet
l	liquid
R	refrigerant
ref	reference greenhouse
w	water
Superscripts	
Design	designed capacity
elec	electricity
inv	investment
Load	heating demand
H	heating
OP	operational
Variables	
A	total heat transfer area ( $m^2$ )
$A_{min}$	min flow area ( $m^2$ )
C	cost (USD)
CP	heat capacity of streams (kW/K)
$c_p$	specific heat capacity ( $kJ/kg \cdot K$ )
d	tube inside diameter (m)
D	tube outside diameter (m)
$D_h$	hydraulic diameter (m)
E	electricity consumption (kWh)
f	friction coefficient
G	mass flux ( $kg/m^2 \cdot s$ )
h	convection heat transfer coefficient ( $W/m^2 \cdot K$ )
k	conduction heat transfer coefficient ( $W/m \cdot K$ )
L	length (m)
$\dot{m}$	mass flow rate (kg/s)
Nu	Nusselt number
Pr	Prandtl number

Q	thermal energy (kWh)
$\dot{Q}$	thermal energy rate (kW)
Re	Reynolds number
t	plate thickness (m)
T	temperature (°C)
U	overall heat transfer coefficient (W/m <sup>2</sup> K)
$\dot{V}$	volumetric flow rate (m <sup>3</sup> /s)
$\dot{W}$	power consumption (kW)
x	saturated vapor quality
Greek letters	
$\beta$	chevron angle, degrees
$\rho$	density (kg/m <sup>3</sup> )
$\eta_{is}$	isentropic efficiency

### Appendix A. Heat Exchanger Models

Various types of heat exchanger are involved in the present study. In this paper, the thermal design and sizing of heat exchangers is accomplished using the LMTD (logarithmic mean temperature difference) method. Figure A1 shows the flowchart describing the process of sizing the heat exchangers. In this method, different thermodynamic models have been developed enabling appropriate sizing of the heat exchanger network. It should be mentioned that a limit of 500 Pa is set on the maximum allowable pressure drop within the AHU and 0.5 bar for the HP cycle. The correlations used to calculate the pressure drop are summarize in Table A1.

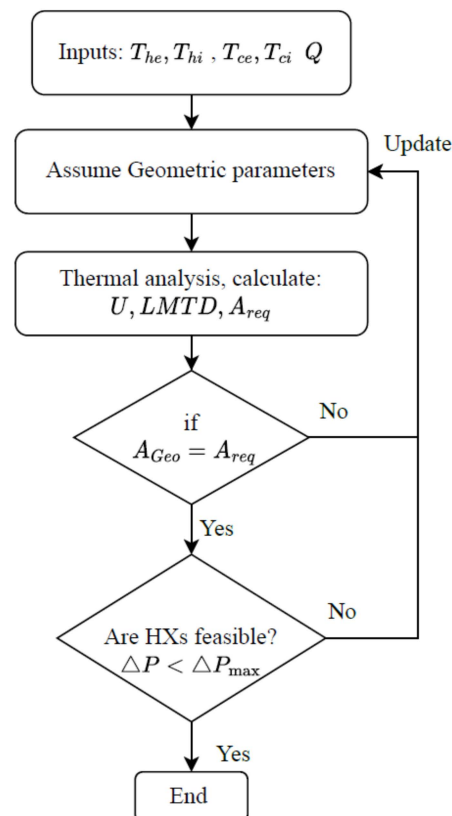


Figure A1. Heat exchangers sizing flowchart.

#### Appendix A.1. Plate Heat Exchangers (PHXs)

In the proposed system, PHXs are used as evaporator and condenser in the HP cycle. The thermodynamic modeling of PHXs experiencing phase change is usually conducted by

dividing the exchanger into single phase and two-phase zones. Each section is designed separately under specified operating conditions according to the log mean temperature difference approach, and the total heat transfer area is calculated accordingly.

#### Appendix A.1.1. Single Phase

For the single-phase flows in PHXs, the  $U$  value can be expressed as:

$$\frac{1}{U} = \frac{1}{h_w} + \frac{t}{k} + \frac{1}{h_R} \quad (\text{A1})$$

where the heat transfer coefficients,  $h$ , are calculated using the Chisholm and Waniarchi [30] correlation:

$$Nu = 0.724 \left( \frac{6\beta}{\pi} \right)^{0.646} Re^{0.583} Pr^{0.33} \quad (\text{A2})$$

$$h = \frac{k}{Nu \cdot D_h} \quad (\text{A3})$$

where  $D_h$  is the hydraulic diameter and  $k$  is the thermal conductivity.

#### Appendix A.1.2. Two-Phase Region

A well-accepted approach for two-phase region modeling is to divide the heat exchanger into a number of smaller regions, in which the fluid properties can be assumed constant. Then, for each region, the overall heat transfer coefficient can be obtained by using Equation (A1). The heat transfer coefficients on the refrigerant side for the evaporator and condenser under two-phase conditions are calculated by the following equations [31]:

$$Nu_{Eva,i} = 1.926 Bo_i^{0.3} Re_i^{0.5} Pr_i^{0.33} \left( 1 - x_i + x_i \left( \frac{\rho_l}{\rho_v} \right)^{0.5} \right) \quad (\text{A4})$$

$$Nu_{Cond,i} = 4.118 Re_i^{0.4} Pr_i^{0.33} \quad (\text{A5})$$

where  $Bo$  is the boiling number and  $x_i$  is the quality of refrigerant for the  $i$ th region [32].

#### Appendix A.2. Air-to-Air Heat Exchangers (AHXs)

Cross-corrugated air-to-air heat exchangers are used as the typical AHX in the present study. For this type of heat exchanger, the heat transfer coefficients are calculated based on the Zhang [33] correlation as follows

$$Nu = 0.274 Re^{0.569} Pr^{0.33} \quad (\text{A6})$$

#### Appendix A.3. Finned-Tube Heat Exchanger (FTHXs)

For finned tube heat exchangers, different correlations are used for the air side and liquid side. The convective heat transfer inside the tubes is estimated by the Gnielinski equation [34]:

$$Nu = \frac{\left( \frac{f}{8} \right) (Re - 1000) Pr}{1 + 12.7 \sqrt{\frac{f}{8}} (Pr^{\frac{2}{3}} - 1)} \quad (\text{A7})$$

$$f = \left( 1.82 \log_{10} Re - 1.64 \right)^{-2} \quad (\text{A8})$$

The heat transfer coefficient of the airflow side of the exchanger can be expressed by the Dias and Young correlation [35].

$$Nu = 0.1378 Re^{0.718} Pr^{0.33} \left( \frac{Y}{H} \right)^{0.296} \quad (\text{A9})$$

The overall heat transfer coefficient is formulated based on the tube outside diameter as follows:

$$U = \frac{1}{\frac{D/d}{h_{in}} + \left( \frac{D \ln\left(\frac{D}{d}\right)}{2k} \right) + \frac{1}{h_{out}\eta_{fin}}} \quad (\text{A10})$$

**Table A1.** The correlations used to calculate pressure drop.

HX Type	Correlation	Ref.
PHX	$\Delta P = f \frac{1}{D} \frac{\rho V_m^2}{2}$ $f = \left[ \frac{0.5 \cos(\beta)}{(0.18 \tan(\beta) + 0.36 \sin(\beta) + f_0 / \cos(\beta))^{0.5}} + \frac{1 - \cos(\beta)}{\sqrt{15.2 f_1}} \right]^{-2}$ $f_0 = 64 / Re$ $f_1 = 597 / Re$	[36]
AHX	$\Delta P = f \frac{1}{D} \frac{\rho V_m^2}{2}$ $f = 6.536 Re^{-0.421}$	[37]
FTHX (over the tube bank)	$\Delta P = \frac{G^2}{2\rho_g} \left[ f \frac{A}{A_{min}} \frac{\rho_g}{\rho_l} + (1 + \sigma^2) \left( \frac{\rho_g}{\rho_l} - 1 \right) \right]$ $\sigma = \frac{\text{minimum free flow}}{\text{frontal area}}$	[38]
FTHX (inside the tubes)	$\Delta P = f \frac{1}{D} \frac{\rho V_m^2}{2}$ $f = \frac{0.064}{Re^{0.2}}$	

## References

- Anifantis, A.S.; Colantoni, A.; Pascuzzi, S. Thermal energy assessment of a small scale photovoltaic, hydrogen and geothermal stand-alone system for greenhouse heating. *Renew. Energy* **2017**, *103*, 115–127. [\[CrossRef\]](#)
- Kristinsson, J. The energy-producing greenhouse. In Proceedings of the PLEA2006—The 23rd Conference on Passive and Low Energy Architecture, Geneva, Switzerland, 6–8 September 2006.
- Rousse, D.R.; Martin, D.; Thériault, R.; Léveillé, F.; Boily, R. Heat recovery in greenhouses: A practical solution. *Appl. Therm. Eng.* **2000**, *20*, 687–706. [\[CrossRef\]](#)
- Gieling, T.H.; Bruins, M.; Campen, J.; Janssen, H.; Kempkes, F.; Raaphorst, M.; Sapounas, A. *Monitoring Technische Systemen in Semi-Gesloten Kassen*; Wageningen UR Greenhouse Horticulture: Wageningen, The Netherlands, 2010.
- Van den Bulck, N.; Coomans, M.; Wittemans, L.; Hanssens, J.; Steppe, K. Monitoring and energetic performance analysis of an innovative ventilation concept in a Belgian greenhouse. *Energy Build.* **2013**, *57*, 51–57. [\[CrossRef\]](#)
- Coomans, M.; Allaerts, K.; Wittemans, L.; Pinxteren, D. Monitoring and energetic performance of two similar semi-closed greenhouse ventilation systems. *Energy Convers. Manag.* **2013**, *76*, 128–136. [\[CrossRef\]](#)
- Maslak, K.; Nimmermark, S. Thermal energy use for dehumidification of a tomato greenhouse by natural ventilation and a system with an air-to-air heat exchanger. *Agric. Food Sci.* **2017**, *26*, 56–66. [\[CrossRef\]](#)
- Fehrm, M.; Reiners, W.; Ungemach, M. Exhaust air heat recovery in buildings. *Int. J. Refrig.* **2002**, *25*, 439–449. [\[CrossRef\]](#)
- Fracastoro, G.V.; Serraino, M. Energy analyses of buildings equipped with exhaust air heat pumps (EAHP). *Energy Build.* **2010**, *42*, 1283–1289. [\[CrossRef\]](#)
- Li, B.; Wild, P.; Rowe, A. Performance of a heat recovery ventilator coupled with an air-to-air heat pump for residential suites in Canadian cities. *J. Build. Eng.* **2019**, *21*, 343–354. [\[CrossRef\]](#)
- Perone, C.; Orsino, M.; La Fianza, G.; Giametta, F.; Catalano, P. Study of a mechanical ventilation system with heat recovery to control temperature in a monitored agricultural environment under Summer conditions. *J. Build. Eng.* **2021**, *43*, 102745. [\[CrossRef\]](#)
- Liu, S.; Ma, G.; Xu, S.; Jia, X.; Wu, G. Experimental study of ventilation system with heat recovery integrated by pump-driven loop heat pipe and heat pump. *J. Build. Eng.* **2022**, *52*, 104404. [\[CrossRef\]](#)
- Smith, R. *Chemical Process: Design and Integration*; John Wiley & Sons: Hoboken, NJ, USA, 2005.
- Misevičiūtė, V.; Motuzienė, V.; Valančius, K. The application of the Pinch method for the analysis of the heat exchangers network in a ventilation system of a building. *Appl. Therm. Eng.* **2018**, *129*, 772–781. [\[CrossRef\]](#)
- Reddick, C.; Sorin, M.; Bonhivers, J.-C.; Laperle, D. Waste heat and renewable energy integration in buildings. *Energy Build.* **2020**, *211*, 109803. [\[CrossRef\]](#)

16. Hosseinnia, S.M.; Sorin, M. A systematic pinch approach to integrate stratified thermal energy storage in buildings. *Energy Build.* **2021**, *232*, 110663. [[CrossRef](#)]
17. Hosseinnia, S.M.; Sorin, M. Energy targeting approach for optimum solar assisted ground source heat pump integration in buildings. *Energy* **2022**, *248*, 123528. [[CrossRef](#)]
18. Ghaderi, M.; Hosseinnia, S.M.; Sorin, M. Assessment of waste heat recovery potential in greenhouse ventilation systems using dynamic pinch analysis. *Appl. Therm. Eng.* **2023**, *227*, 120363. [[CrossRef](#)]
19. Ahamed, M.S.; Guo, H.; Tanino, K. A quasi-steady state model for predicting the heating requirements of conventional greenhouses in cold regions. *Inf. Process. Agric.* **2018**, *5*, 33–46. [[CrossRef](#)]
20. Yang, P.; Liu, L.-l.; Du, J.; Li, J.-l.; Meng, Q.-w. Heat exchanger network synthesis for batch processes by involving heat storages with cost targets. *Appl. Therm. Eng.* **2014**, *70*, 1276–1282. [[CrossRef](#)]
21. Kemp, I.C. *Pinch Analysis and Process Integration: A User Guide on Process Integration for the Efficient Use of Energy*; Elsevier: Amsterdam, The Netherlands, 2011.
22. Kavanaugh, S.P. Design of geothermal systems for commercial and institutional buildings. In *Ground-Source Heat Pumps*; ASHRE: New York, NY, USA, 1997.
23. Wang, B.; Arsenyeva, O.; Zeng, M.; Klemeš, J.J.; Varbanov, P.S. An advanced Grid Diagram for heat exchanger network retrofit with detailed plate heat exchanger design. *Energy* **2022**, *248*, 123485. [[CrossRef](#)]
24. Xu, Y.; Mao, C.; Huang, Y.; Shen, X.; Xu, X.; Chen, G. Performance evaluation and multi-objective optimization of a low-temperature CO<sub>2</sub> heat pump water heater based on artificial neural network and new economic analysis. *Energy* **2021**, *216*, 119232. [[CrossRef](#)]
25. Hsieh, J.-C.; Lai, C.-C.; Chen, Y.-H. Thermoeconomic analysis of a waste heat recovery system with fluctuating flue gas scenario. *Energy* **2022**, *258*, 124866. [[CrossRef](#)]
26. Le Roux, D.; Olivès, R.; Neveu, P. Geometry optimisation of an industrial thermochemical Thermal Energy Storage combining exergy, Life Cycle Assessment and Life Cycle Cost Analysis. *J. Energy Storage* **2022**, *55*, 105776. [[CrossRef](#)]
27. Robert, F.; Gosselin, L. New methodology to design ground coupled heat pump systems based on total cost minimization. *Appl. Therm. Eng.* **2014**, *62*, 481–491. [[CrossRef](#)]
28. Ghamari, V.; Hajabdollahi, H.; Dehaj, M.S.; Saleh, A. Investigating the effect of energy storage tanks on thermoeconomic optimization of integrated combined cooling, heating and power generation with desalination plant. *J. Energy Storage* **2022**, *56*, 106120. [[CrossRef](#)]
29. Sagani, A.; Vrettakos, G.; Dedoussis, V. Viability assessment of a combined hybrid electricity and heat system for remote household applications. *Sol. Energy* **2017**, *151*, 33–47. [[CrossRef](#)]
30. Chisholm, D.; Wanniarachchi, A. Plate heat exchangers: Plate selection and arrangement. In Proceedings of the AIChE Meeting, Orlando, FL, USA, 18–22 March 1990.
31. Li, R.; Wang, H.; Yao, E.; Zhang, S. Thermo-economic comparison and parametric optimizations among two compressed air energy storage system based on Kalina cycle and ORC. *Energies* **2016**, *10*, 15. [[CrossRef](#)]
32. Imran, M.; Usman, M.; Park, B.-S.; Kim, H.-J.; Lee, D.-H. Multi-objective optimization of evaporator of organic Rankine cycle (ORC) for low temperature geothermal heat source. *Appl. Therm. Eng.* **2015**, *80*, 1–9. [[CrossRef](#)]
33. Zhang, L.-Z. Numerical study of periodically fully developed flow and heat transfer in cross-corrugated triangular channels in transitional flow regime. *Numer. Heat Transf. Part A Appl.* **2005**, *48*, 387–405. [[CrossRef](#)]
34. Gnielinski, V. New equations for heat and mass transfer in turbulent pipe and channel flow. *Int. Chem. Eng.* **1976**, *16*, 359–368.
35. Wang, Z.; Hu, Y.; Xia, X.; Zuo, Q.; Zhao, B.; Li, Z. Thermo-economic selection criteria of working fluid used in dual-loop ORC for engine waste heat recovery by multi-objective optimization. *Energy* **2020**, *197*, 117053. [[CrossRef](#)]
36. Chatzopoulou, M.A.; Lecompte, S.; De Paepe, M.; Markides, C.N. Off-design optimisation of organic Rankine cycle (ORC) engines with different heat exchangers and volumetric expanders in waste heat recovery applications. *Appl. Energy* **2019**, *253*, 113442. [[CrossRef](#)]
37. Liang, C.; Tong, X.; Lei, T.; Li, Z.; Wu, G. Optimal design of an air-to-air heat exchanger with cross-corrugated triangular ducts by using a particle swarm optimization algorithm. *Appl. Sci.* **2017**, *7*, 554. [[CrossRef](#)]
38. Wang, C.-C. Recent progress on the air-side performance of fin-and-tube heat exchangers. *Int. J. Heat Exch.* **2000**, *1*, 49–76.

**Disclaimer/Publisher's Note:** The statements, opinions and data contained in all publications are solely those of the individual author(s) and contributor(s) and not of MDPI and/or the editor(s). MDPI and/or the editor(s) disclaim responsibility for any injury to people or property resulting from any ideas, methods, instructions or products referred to in the content.